International Food Research Journal 29(6): 1401 - 1410 (December 2022)
Journal homepage: *http://www.ifrj.upm.edu.my*

Modelling of the kinetics of red tilapia (*Oreochromis* spp.) viscera enzymatic hydrolysis using mathematical and neural network models

[1]*Álvarez, A. C., [2]Sepúlveda, T. and [2]Zapata, J. É.

[1]*Departamento de Ingeniería Química, Facultad de Ingeniería, Universidad de Antioquia, Calle 67 # 53-108, Medellín, Colombia*
[2]*Grupo de Investigación "Nutrición y Tecnología de Alimentos", Universidad de Antioquia, Calle 70 #52-21, Medellín, Colombia*

Article history

Received:
5 March 2021
Received in revised form:
29 March 2022
Accepted:
30 May 2022

Keywords

enzymatic hydrolysis,
Oreochromis spp.,
kinetic model,
neural network

Abstract

The present work modelled the enzymatic hydrolysis of red tilapia (*Oreochromis* spp.) viscera with Alcalase® 2.4 L in both 0.5 and 5 L reactors. The best conditions for the enzymatic hydrolysis were 60°C and pH 10. The product inhibited the enzymatic hydrolysis, and the enzyme deactivated following second-order reaction. K_M and K_p from a secondary plot of K_M^{app} as a function of inhibitor concentration, and k_2, p, and k_3 were found by non-linear regression. While the obtained parameters modelled the 0.5 L reactor well, it did not model the 5 L reactor, probably because of unconsidered fluid dynamics in the model. To have a better modelling, a neural network (tensorflow.keras.models module) was built and trained. The neural network modelled the enzymatic hydrolysis of red tilapia at several concentrations of substrate and enzyme. This result proved that neural networks are a powerful tool for modelling biological processes.

DOI
https://doi.org/10.47836/ifrj.29.6.16

Introduction

The growing consumer interest in natural and healthy foods has intensified. Bioactive peptides are currently a focus of research because they have shown multiple biological properties that natural processes can provide (Dullius *et al.*, 2020). Enzymatic hydrolysis is a process that allows for breaking the peptide bonds that modify the structure of proteins (Wu *et al*., 2020). Enzymatic hydrolysates are obtained under controlled conditions of pH, temperature, and hydrolysis time. Enzymes such as trypsin, pepsin, chymotrypsin, papain, as well as industrial food-grade proteinases including Protamex™, Alcalase®, and Flavourzyme® from microorganisms have been widely applied (Samaranayaka and Li-Chan, 2011).

Establishing a kinetic model for the enzymatic hydrolysis of proteins is a complex endeavour since classical models such as the Michaelis-Menten kinetics misrepresent the mechanism (Qi and He, 2006). To improve the models based on Michaelis-Menten approach, Marquez Moreno and Fernandez Cuadrado (1993) proposed a kinetic model involving substrate inhibition and second-order enzymatic deactivation that was modified by González-Tello *et al.* (1994). Later, Qi and He (2006) included substrate, product inhibition, and enzyme inactivation, then developed full deductions and mechanisms, which later on were modified by Valencia *et al.* (2019).

Modelling the enzyme deactivation is challenging (Gálvez *et al.*, 2016) due to the complexity of the reactions involved. Response surface methodology has been used to model enzymatic hydrolysis, but for biological systems, polynomials fail to model, in some cases, the complete system (Morales-Medina *et al.*, 2016). Furthermore, when modelling large volume reactors (*i.e.*, 5 L), the fluid dynamics such as stirring speed, heat transfer, mass transfer, viscosity, and turbidity need to be considered to predict the data accurately. Therefore, it could result in an overly complex system of equations.

*Corresponding author.
Email: acamilo.alvarez@udea.edu.co

Artificial neural networks (ANN) are an alternative to modelling enzymatic hydrolysis since they predict values of the product regarding input conditions without considering parameters from the kinetics (Corazza *et al*., 2005). ANN consist of connected units or nodes through an input layer, one or more hidden layers, and an output layer. With some specific algorithms, ANN are capable of learning any mathematical function with sufficient training data (Aggarwal, 2018). They have been applied in the modelling of biological systems (Castro *et al.,* 2010; Das *et al.,* 2015; Gálvez *et al.,* 2016; Morales-Medina *et al.,* 2016).

The present work thus aimed to apply a model previously proposed by Qi and He (2006) and modified by Valencia *et al.* (2019) to the enzymatic hydrolysis of red tilapia viscera in a small reactor (0.5 L), and find the kinetic constants based on the mechanism observed under typical operating conditions; also, to model the enzymatic hydrolysis of red tilapia viscera in a larger reactor (5 L) via the neural network approach to improve the goodness of fit parameters.

Materials and methods

Materials management

Fresh red tilapia (*Oreochromis* spp.) viscera were provided by Piscícola el Gaitero in Sopetrán at 750 MASL, Colombia. The viscera were packed in polyethylene bags, and kept in ice during transportation. Upon arrival at the laboratory, the tilapia viscera were minced using a blender, and heated at 90°C for 20 min to inactivate endogenous enzymes. The tilapia viscera were then stored in a plastic vessel at -20°C. After 24 h, the fat was separated from the viscera, and then removed by cutting the frozen block with a knife. The defatted viscera remained at -20°C until further use. The protein content of viscera was measured by the Kjeldahl method using a conversion factor of 6.25 (AOAC, 2005).

Catalytic activity of Alcalase® 2.4 L

The proteolytic activity of Alcalase® 2.4 L was determined following the Anson method with slight modifications (Vasquez and Zapata Montoya, 2018). Tilapia viscera or casein (600 µL) was mixed with 60 µL of the enzyme. The mixture was incubated at the experimental design temperature for 10 min. The reaction was stopped by the addition of 600 µL of 110 mM TCA. The mixture was centrifuged at 10,000 rpm for 2 min, and 300 µL of the supernatant was mixed with 750 µL of 0.5 M Na_2CO_3 and 150 µL of the 0.5 M Folin reagent. The mixture was incubated at 37°C for 30 min, and the absorbance was measured at 660 nm. The standard curve of tyrosine allowed the amount in micromoles of tyrosine equivalents released from casein per minute to be calculated.

Effect of pH and temperature on the catalytic activity of Alcalase® 2.4 L

To establish the optimal pH and temperature conditions of the enzyme Alcalase® 2.4 L (Novozymes, Denmark) in the catalytic activity of the red tilapia viscera substrate, a central composite design was performed with varying pH (8, 9, and 10) and temperature (40, 50, and 60°C) levels. The analysis of variance (ANOVA) from Design-Expert® Software (Stat-Ease, Inc., USA) was used to assess the significance of the regression coefficients, and to predict the best conditions of pH and temperature.

Enzymatic hydrolysis of red tilapia viscera

The enzymatic hydrolysis of red tilapia viscera was conducted in a jacketed vessel at pH 10 at 60°C. The reaction was started by adding Alcalase® 2.4 L (Novozymes, Denmark) at an enzyme/substrate (E/S) ratio of 10% (w/w, wet weight) with 4.6 units of enzymatic activity per gram of protein. The hydrolysis was controlled using a pH-stat by adding a 2 N NaOH solution using a TitroLine@ 7000 (Xylem Analytics, Germany) for the 0.5 L reaction, and a Bioflo 310® (New Brunswick Scientific Co., Inc. USA) for the 5 L reaction, for 60 and 175 min, respectively. The enzyme was inactivated by heating at 90°C for 10 min. The hydrolysate was centrifuged at 4,500 *g* (Heraeus Multifuge 3L, Labcare Ltd., Buckinghamshire, England) for 30 min at 4°C. The supernatant (tilapia hydrolysate) was stored at -20°C until further experiments. The degree of hydrolysis was calculated according to Valencia *et al.* (2014) in terms of the released amino groups using Eq. 1:

$$\alpha\text{–NH (mM)} = \frac{B \cdot N}{\alpha \cdot V} \quad \text{(Eq. 1)}$$

where, B = volume (L) of NaOH added, N = NaOH concentration (mM), V = processing volume (L), and α = average degree of dissociation of the α–NH groups calculated from Eq. 2 and 3:

$$\alpha = \frac{10^{pH-pK}}{1+10^{pH-pK}} \quad \text{(Eq. 2)}$$

$$pK = 7.8 + \frac{298-T}{298 \cdot T} \cdot 2400 \quad \text{(Eq. 3)}$$

Effect of substrate concentration and product addition on the reaction

Enzymatic hydrolysis at different substrate concentrations (between 45.5 – 354 mM) was conducted to evaluate the effect of the substrate on the behaviour of reaction rate. Furthermore, three concentrations of hydrolysate (0, 4, and 20 mM), which were added before starting the hydrolysis, were used to evaluate the hypothesis of product inhibition. The hydrolysis conditions were at pH 10 and 60°C, and the addition of the base was controlled via the pH-stat method.

Thermal inactivation of Alcalase®

The effect of temperature on the enzymatic activity of Alcalase® was evaluated at different temperatures (50, 60, and 70°C) under reactive conditions. The experiments were performed at a substrate concentration of 91 mM and pH 10. Once the desired temperature was reached, Alcalase® was added to the substrate, and samples were collected each 30 min for 210 min. The proteolytic activity of Alcalase® 2.4 L was determined following the procedure described in the catalytic activity of Alcalase® 2.4 L. The relative activity was calculated as a relation between the activity at time *t* with respect to the initial activity. The data were plotted and analysed to find the inactivation constant.

Modelling and determination of kinetic parameters by fitting

The degree of hydrolysis (DH) is a standard parameter to control the hydrolysis. It is the percentage of peptides bonds cleaved, which can be measured by the pH-stat technique based on the following principles (Adler-Nissen *et al.*, 1983):

Opening of peptide bond:

$$-\mathrm{CHR'-CO-NH-CHR''-} + \mathrm{H_2O} \xrightarrow{\text{Enzyme}} -\mathrm{CHR'-COOH} + \mathrm{NH_2-CHR''}$$

Proton exchange:

$$-\mathrm{CHR'-COOH} + \mathrm{NH_2-CHR''} \longrightarrow -\mathrm{CHR'-COO^-} + \mathrm{NH_3^+-CHR''}$$

Titration of amino group:

$$\mathrm{NH_3^+-CHR''} + \mathrm{OH^-} \rightleftharpoons \mathrm{NH_2-CHR''} + \mathrm{H_2O}$$

Each cleaved peptide bond forms one free amino group and one free carboxyl group. By adding a basic solution, the pH is kept constant, and the quantity of base is proportional to the number of peptide bonds cleaved.

Marquez Moreno and Fernandez Cuadrado (1993) obtained an expression (Eq. 4) in terms of the DH based on the general mechanism as follows:

$$\mathrm{E + S} \underset{k_{-1}}{\overset{k_1}{\rightleftharpoons}} \mathrm{ES} \xrightarrow{k_2} \mathrm{E + P}$$

$$\frac{d(DH)}{dt} = ae^{-b(DH)} \quad \text{(Eq. 4)}$$

The inactivation mechanism of protease during hydrolysis is described by:

$$\mathrm{E + ES} \xrightarrow{k_3} \mathrm{E_A + E_I + P}$$

By including the substrate and product inhibition as well as enzyme inactivation, Qi and He (2006) developed full deductions and mechanisms where the *a* and *b* from Eq. 4 are kinetic constants, and can be replaced by different expressions based on the reaction mechanism. Those expressions can be useful since several authors proved the effects of substrate inhibition (González-Tello *et al.*, 1994; Márquez and Vázquez, 1999; Qi and He, 2006) and product inhibition (Demirhan *et al.*, 2011; Valencia *et al.*, 2014) as the following reactions:

$$\mathrm{S + ES} \underset{k_{-4}}{\overset{k_4}{\rightleftharpoons}} \mathrm{SES}$$

$$\mathrm{E + P} \underset{k_{-5}}{\overset{k_5}{\rightleftharpoons}} \mathrm{EP}$$

Recently, Valencia *et al.* (2019) modified Eq. 4 into an expression in terms of product concentration instead of the degree of hydrolysis as Eq. 5 shows:

$$\frac{dP}{dt} = ae^{-bP} \;\therefore\; P = \frac{1}{b}\ln(abt+1) \quad \text{(Eq. 5)}$$

For the product inhibition mechanism, the values of the parameters *a* and *b* correspond to Eqs. 6

and 7, respectively. Where k_2, K_p, K_m, and k_3 are parameters that must be determined; however, calculating exact values of these parameters is a difficult task since there are many of them to estimate.

$$a = \frac{k_2 e_0 s_0 K_p}{K_m p + K_p s_0} \quad \text{(Eq. 6)}$$

$$b = \frac{k_3 K_m K_s}{k_2 (K_m p + K_p s_0)} \quad \text{(Eq. 7)}$$

In the present work, all the parameters were fitted using the *curve_fit* function of the SciPy.optimize module in python. It uses non-linear least squares to fit a function to data by using the Trust Region Reflective method for constrained problems. The boundaries of the parameters were [0, inf], and the starting values 1.0. R^2 and χ^2 were used to evaluate the goodness of fit (Eqs. 8 and 11, respectively). Where SS_{res} was the sum of squares of residuals (Eq. 9), and SS_{tot} was the total sum of squares (Eq. 10), in which y_i were the actual values, $\hat{y}_i$ were the predicted values, and $\bar{y}$ was the mean value; N was the number of parameters to fit. R^2 around 1.0, and χ^2 around 0 determine a good fit of the experimental data.

$$R^2 = 1 - \frac{SS_{res}}{SS_{tot}} \quad \text{(Eq. 8)}$$

$$SS_{res} = \sum_i (y_i - \hat{y}_i)^2 \quad \text{(Eq. 9)}$$

$$SS_{tot} = \sum_i (y_i - \bar{y})^2 \quad \text{(Eq. 10)}$$

$$\chi^2 = \frac{SS_{res}}{N} \quad \text{(Eq. 11)}$$

Artificial neural network

An artificial neural network is a mathematical model to predict values by training a dataset. It is a network of interconnected units or elements called neurons (Haykin, 1999). It consists of an input layer, one or more hidden layers, and an output layer (Svozil *et al.*, 1997). In the input layer, a function concerning weights (w) and biases (b) (Eq. 12) is applied to the features for all the training examples. In the hidden layer, an activation function is applied to pass to the output layer, in which the new data are applied to another activation function to calculate the predicted values that are passed to a loss function. Based on the value of the loss function, the algorithm makes calculations and goes in the opposite direction to the input layer to update the values of weights and biases.

$$Z = wX + b \quad \text{(Eq. 12)}$$

The architecture of the neural network selected for the modelling of the enzymatic hydrolysis of red tilapia viscera consisted of an input layer, a hidden layer, and an output layer. The input features were S_0, e_0, and t, so the input layer consisted of three units interconnected to one hidden layer. The hidden layer consisted of 10 units which have been demonstrated to work very well in modelling enzymatic hydrolysis (Gálvez *et al.*, 2016; Morales-Medina *et al.*, 2016). The activation function for the hidden layer was the *tanh* function that returned values between -1 and 1 following Eq. 13. For the output layer, the *relu* (rectifier linear unit) activation function (Eq. 14) was used, which is suitable for regression problems. The cost function was the mean squared error (Eq. 15), in which n was the number of training examples, y_i were the actual values of the training examples, and $\hat{y}_i$ were the predicted values from the neural network.

$$\tanh(z) = \frac{e^z - e^{-z}}{e^z + e^{-z}} \quad \text{(Eq. 13)}$$

$$a = \max(0, z) \quad \text{(Eq. 14)}$$

$$MSE = \frac{1}{n}\sum_{i=1}^{n}(y_i - \hat{y}_i)^2 \quad \text{(Eq. 15)}$$

The Adam optimiser (Kingma and Ba, 2015) — an efficient algorithm that is gaining popularity (Bansal *et al.*, 2016; Peng *et al.*, 2018; Chang *et al.*, 2019) was used to update the network weights in an iterative process. To train the neural network, 100 epochs that are the number of iterations or passes through the training dataset were used. The batch size was one; it means that the algorithm iterates in group samples of one. The data were pre-processed with the MinMaxScaler function from the sklearn.preprocessing module, which transformed the input features to the range of 0 - 1. Also, the data were split into 70% for training and 15% for testing with the train_test_split function from the sklearn.model_selection, while the remaining 15% were selected for final validation.

Results and discussion

Effect of pH and temperature on the catalytic activity of the enzyme

A central composite design to study the effect of the temperature (T) and pH on the catalytic activity

of Alcalase® in the presence of red tilapia viscera was used. The *p*-values being lower than 0.005 showed that the temperature and pH had a statistically significant effect on the activity of the enzyme, with both variables having a positive effect. The surface response methodology indicated that the conditions that maximise activity were pH 10 and temperature 60°C.

The conditions of enzymatic hydrolysis affect the properties of the generated hydrolysates. In accordance with the specificity of enzymes, they catalyse the hydrolysis of specific peptide bonds in proteins (Dermiki and FitzGerald, 2020). Proteinases have optimal pH and temperature values that should be controlled during hydrolysis. Alcalase® is a serine protease produced by *Bacillus licheniformis* with a typical pH range of 6 - 10, with the manufacturer reporting that the optimum pH can be found at 10 with remarkable stability at alkaline pH values, and an optimal temperature range of 50 - 60°C (Adler-Nissen, 1993; González-Tello *et al.,* 1994; Tacias-Pascacio *et al.*, 2020), which agrees with the values of pH and temperature found in the present work. An optimal pH value of 9.5 was found in a study conducted on tilapia viscera using Alcalase® (Baez-Suarez *et al.*, 2016).

Other studies have reported hydrolysis at 60°C with the same enzyme such as the enzymatic hydrolysis of Nile tilapia (*O. niloticus*) skeleton flour (Borges-Contreras *et al.,* 2019), bovine plasma hydrolysis (Gómez Sampedro and Zapata Montoya, 2016), hydrolysis of rainbow trout viscera (Vasquez and Zapata Montoya, 2018), hydrolysis of flaxseed (*Linum usitatissimum*) protein (Silva *et al.,* 2017), and hydrolysis of tilapia (*O. niloticus*) by-product (Roslan *et al.,* 2014). The optimal conditions (pH 10, 60°C) were used for the subsequent experiments.

Effect of substrate concentration and product addition on the reaction

Figure 1a shows the saturation curve for the enzymatic hydrolysis of red tilapia viscera. The reaction rate increased as the substrate concentration increased; however, from 220 mM, the enzyme became saturated with substrate. Since the reaction rate remained constant in this range of concentration, the inhibition by substrate was ruled out in the concentration range of the substrate studied. The kinetic parameters K_M and V_{max}, obtained by a non-linear fit, were 118.7 mM and 2.5 mM/min, respectively. These values were higher than those found in cheese whey hydrolysates, whey hydrolysates (Sousa *et al.,* 2004), and salmon (*Salmo salar*) muscle hydrolysates (Valencia *et al.,* 2014). Those studies also used Alcalase® as an enzyme.

Finding the initial velocity while varying substrate concentration and product concentration helps to evaluate the hypothesis of inhibition by product. Results showed that as the concentration of hydrolysate (inhibitor) increased, the initial rates decreased. When fixing the inhibitor concentration, the values of K_M^{app} and V_{max}^{app} were obtained with a non-linear curve-fitting from Michaelis-Menten equation (Eq. 16):

$$v = V_{max}\left(\frac{1}{1+\frac{K_M}{[S]}}\right) \quad \text{(Eq. 16)}$$

The values of K_M^{app} and V_{max}^{app} were used in the reciprocal Eq. 17 to obtain a linear function for each concentration of inhibitor. The double-reciprocal plots (Figure 1b) are useful to determine the modality of inhibition from the pattern of lines. The pattern of the straight lines with the competitive inhibitor.

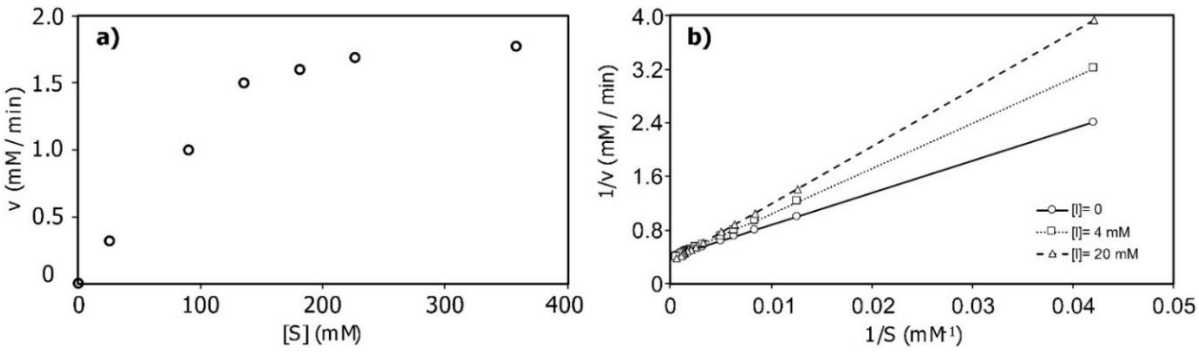

Figure 1. (a) Saturation curve for Alcalase® showing the relation between the concentration of tilapia viscera and reaction rate, and **(b)** double-reciprocal plot for the effect of the inhibitor on the velocity.

These results were coherent because both the substrate and the product had the same structural nature, and therefore, they might have bound to the enzyme at the same active site. The values of K_I and K_M were obtained from a secondary plot of K_M^{app} as a function of inhibitor concentration [I]. The *x*-intercept is equal to the negative value of the K_I, and the *y* intercept is equal to K_M (Copeland, 2000).

$$\frac{1}{v} = \left(\frac{K_M}{V_{max}}\frac{1}{[S]}\right) + \frac{1}{V_{max}} \quad \text{(Eq. 17)}$$

The values of K_I and K_M were 22.38 and 134.7 mM, respectively. K_I was lower than K_M, which is characteristic of competitive inhibition. In this type of inhibition, an inhibitor competes with the substrate for the active site of the enzyme. In common hydrolysis conditions, the peptide products of hydrolysis become substrates which favour a competition between the original substrate and the peptides (Adler-Nissen, 1993). These results could suggest a preference of the enzyme for smaller peptides, since it was expected that the peptides from the hydrolysate would be smaller than those from the substrate. Other studies have also suggested inhibition by product. For example, González-Tello *et al.* (1994) proposed that the decrease observed in the rate of hydrolysis of whey proteins could be due to an inhibition by the products of hydrolysis. Sousa *et al.* (2004) concluded that a kinetic model with competitive inhibition by product presented a better fit for its experimental data on the hydrolysis of whey protein by Alcalase®. Similarly, Demirhan *et al.* (2011) found that the hydrolysis of sesame cake protein by Alcalase® exhibited product inhibition. Valencia *et al.* (2014) found an inhibition by hydrolysis products in the hydrolysis of salmon muscle. They concluded that this inhibition handles the typical shape of the hydrolysis curve.

Thermal inactivation

The thermal inactivation of the enzyme during hydrolysis was studied at three temperatures (50, 60, and 70°C) in the presence of red tilapia viscera (91 mM). Figure 2 shows that the increase in the hydrolysis temperature decreases the activity of the enzyme. At 50°C, the enzyme kept its activity for 180 min; however, at 60°C, the activity after 180 min was 50% less. On the other hand, at 70°C, the inactivation of the Alcalase® was faster and fell dramatically after 30 min. Thermal inactivation of the enzyme at 60°C had the best fit with second-order inactivation kinetics with an R^2 of 0.99. This result agrees with several studies that suggest that the inactivation of the enzyme during hydrolysis is a second-order reaction (Marquez Moreno and Fernandez Cuadrado, 1993; González-Tello *et al.*, 1994; Qi and He, 2006).

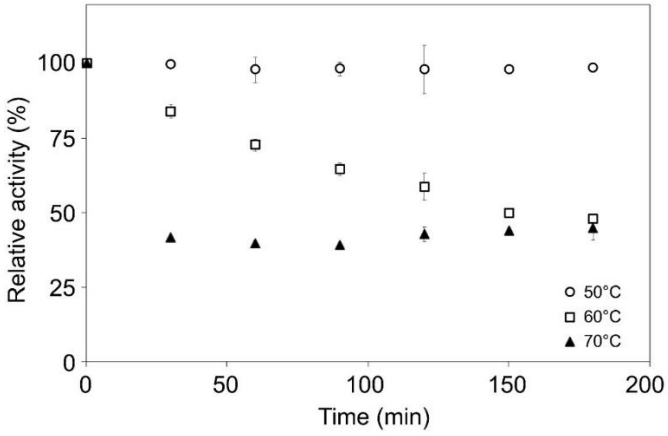

Figure 2. Thermal inactivation of Alcalase® at 50, 60, and 70°C. Error bars represent the standard deviation (n = 3).

Determination of kinetic parameters

Eq. 5 (Valencia *et al.*, 2014) was selected to determine the kinetic parameters of red tilapia viscera enzymatic hydrolysis, based on the findings in the product inhibition and enzyme inactivation obtained in the present work. The K_I and K_M values calculated previously were used as known constants in the model to decrease the number of parameters to estimate. K_I represents K_p in Eqs. 6 and 7, since it corresponds to the inhibition by product. For the 0.5 L reactor, the best set of parameters that acceptably modelled all the curves of red tilapia viscera were k_2 = 5.36 mM·L/min·g, p = 0.75 mM, and k_3 = 3.13 L/g·min (Figure 3), with an R^2 of 0.928, 0.992, and 0.983 for 45.5, 91.0, and 136.5 mM, respectively. These results showed that the product inhibition mechanism described the experimental data in the concentration range of the evaluated substrate.

When performing the same procedure to the reactor of 5 L, it was found that the model from Eq. 5 did not fit the model with just one set of kinetic parameters, even using the same hydrolysis conditions and substrate concentration ranges as in the smaller reactor. However, parameters *a* and *b* were estimated, and are shown in Table 1. For that reason, the enzymatic hydrolysis of red tilapia viscera in a 5 L reactor was modelled with a neural network

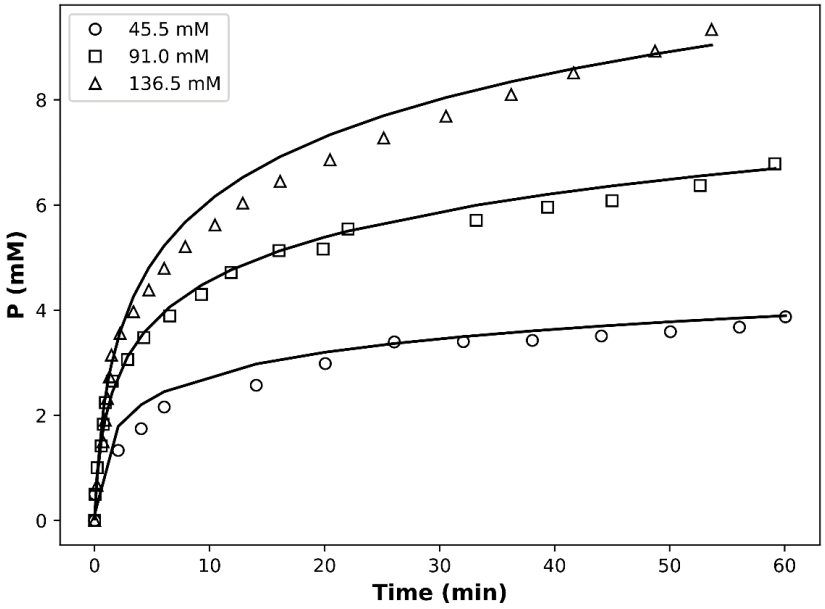

Figure 3. Hydrolysis reaction at different substrate concentrations of red tilapia viscera in a 0.5 L reactor using 1 g/L Alcalase®, pH 10, and 60°C. Data points are the experimental values, and continuous lines are the fitted model according to Eq. 5.

Table 1. Parameters obtained in the fitting of the enzymatic hydrolysis of red tilapia viscera in a 0.5 L reactor.

s_0 (mM)	e_0 (g/L)	a	b	R^2	χ^2
10	1	12.673	1.433	0.711	0.168
10	2	43.198	0.865	0.622	0.833
10	3	14.539	0.387	0.96	0.835
30	3	9.957	0.185	0.995	0.162
40	3	6.464	0.159	0.998	0.082

approach. Neural networks can model biological processes such as enzymatic reactions, represent non-linear relationships, and estimate the response based on trained data (Ba and Boyaci, 2007; Gálvez *et al.*, 2016; Morales-Medina *et al.*, 2016).

Artificial neural network

All the programming was made in Python 3.7 — a general-purpose, open-source programming language — Keras, which is a high-level application programming interface of TensorFlow 2 was used for developing deep learning models. Specifically, the sequential class of the module tensorflow.keras.models was used to build and train the neural network. For the experiments, the enzyme concentration ranged from 1 - 3 g/L, with the substrate concentration from 10 - 40 mM, and reaction time of 180 min for all the enzymatic hydrolysis. This gave a total of 7,668 data points to train and validate the ANN.

The mean square error of the neural network training after the 100 epochs was 2×10^{-4} for both the train and test datasets (Figure 4a), which is acceptable for the values of products in the enzymatic hydrolysis. Das *et al*. (2015) set a value of 5×10^{-4} for the modelling of the enzymatic saccharification of water hyacinth biomass for ethanol, and found that a neural network reached that value. Figure 4b shows that the predicted values agreed with the experimental ones. It corresponded to an R^2 of 0.999, which proved the excellent behaviour of the artificial neural network. The R^2 of the training set was 0.999, which was similar to that obtained for the test set, and confirmed that there was no overfitting of the training dataset.

The results obtained in the present work are similar to that reported in the literature concerning biological systems. To name a few, Chang *et al.* (2011) modelled the enzymatic hydrolysis of steam-exploded Napier grass, and found that a neural network (R^2 = 0.988) performed better than both multiple linear regression and partial least-square regression. Das *et al.* (2015) found that a neural network with an R^2 of 0.9996 had higher accuracy than the surface response methodology. Das *et al.* (2015) found an R^2 value of 0.9987 for a neural network in the modelling of the production of blood protein hydrolysates for plant fertilisation. Morales-

Medina *et al.* (2016) found an R^2 of 0.978 in the modeling of the enzymatic hydrolysis of horse mackerel (*Trachurus mediterraneus*) protein using protease.

The high R^2 and low mean square error found in the present work make neural networks suitable for the modelling of the enzymatic hydrolysis of red tilapia viscera, at substrate and enzyme concentrations in the range of 10 - 40 mM and 1 - 3 g/L, respectively.

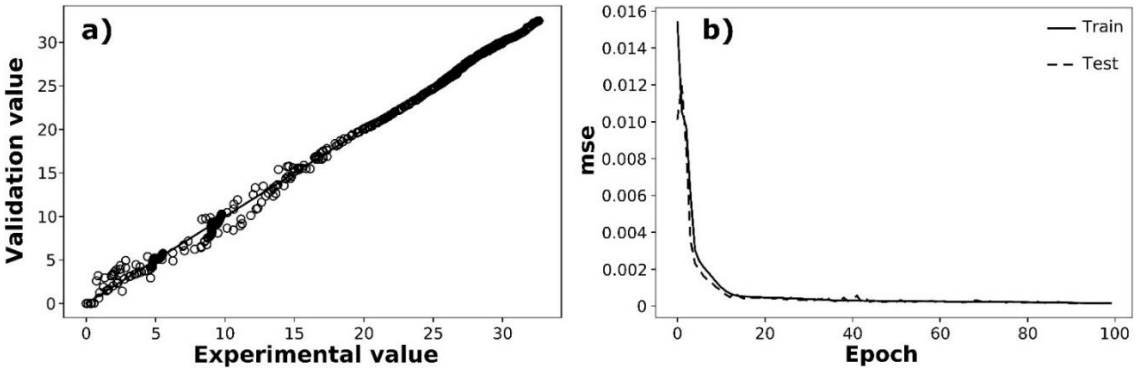

Figure 4. Neural network results: **(a)** experimental and predicted concentration of product from the validation values, and **(b)** mean square error for the neural network up to 100 epochs.

Conclusion

Temperature and pH affected the catalytic activity of the enzymatic hydrolysis reaction of red tilapia (*Oreochromis* spp.) viscera. The reaction presented competitive inhibition by the product (new peptides released from hydrolysis). At temperatures above 60°C, the Alcalase® enzyme was deactivated following second-order kinetics. Kinetic models could predict the behaviour of the enzymatic hydrolysis of red tilapia viscera with Alcalase® in a 0.5 L reactor. However, they failed in modelling the hydrolysis in 5 L reactors. In a 5 L reactor, an artificial neural network approach behaved better, thus suggesting that this kind of model could be suitable for predicting enzymatic hydrolysis in larger reactors.

Acknowledgement

The authors are grateful for the financial support provided by Comité para el Desarrollo de la Investigación en la Universidad de Antioquia (CODI) through the sustainability program and COLCIENCIAS through call 647.

References

Adler-Nissen, J. 1993. Chapter 7 - proteases. In Nagodawithana, T. and Reed, G. (eds). Enzymes in Food Processing, p. 159-203. United States: Academic Press.

Adler-Nissen, J., Eriksen, S. and Olsen, H. S. 1983. Improvement of the functionality of vegetable proteins by controlled enzymatic hydrolysis. Qualitas Plantarum Plant Foods for Human Nutrition 32(3-4): 411-423.

Aggarwal, C. C. 2018. Neural networks and deep learning. 1st ed. United States: Springer.

Association of Official Analytical Chemist (AOAC). 2005. Official methods of analysis of AOAC International. 18th ed. United States: AOAC.

Ba, D. and Boyaci, I. H. 2007. Modeling and optimization II: Comparison of estimation capabilities of response surface methodology with artificial neural networks in a biochemical reaction. Journal of Food Engineering 78(3): 846-854.

Baez-Suarez, J. A., Ospina de Barreneche, N. and Zapata Montoya, J. E. Z. 2016. Effect of temperature, pH, substrate concentration and type of enzyme on the enzymatic hydrolysis of viscera of red tilapia (*Oreochromis* spp.). Información Tecnológica 27(6): 63-76.

Bansal, T., Belanger, D. and McCallum, A. 2016. Ask the GRU: Multi-task learning for deep text recommendations. In RecSys 2016 - Proceedings of the 10th ACM Conference on Recommender Systems. Boston, United States.

Borges-Contreras, B., Martínez-Sánchez, C. E., Herman-Lara, E., Rodríguez-Miranda, J., Hernández-Santos, B., Juárez-Barrientos, J. M., … and Torruco-Uco, J. G. 2019. Angiotensin-converting enzyme inhibition *in*

vitro by protein hydrolysates and peptide fractions from mojarra of Nile tilapia (*Oreochromis niloticus*) skeleton. Journal of Medicinal Food 22(3): 286-293.

Castro, E., Cara, C., Jesus, M. J. and Rivas, V. 2010. Comparison of response surface methodology and artificial neural network applied to enzymatic hydrolysis of rapeseed straw. Journal of Biotechnology 150: 137-137.

Chang, C. W., Yu, W. C., Chen, W. J., Chang, R. F. and Kao, W. S. 2011. A study on the enzymatic hydrolysis of steam exploded napiergrass with alkaline treatment using artificial neural networks and regression analysis. Journal of the Taiwan Institute of Chemical Engineers 42(6): 889-894.

Chang, Z., Zhang, Y. and Chen, W. 2019. Electricity price prediction based on hybrid model of adam optimized LSTM neural network and wavelet transform. Energy 187: 115804.

Copeland, R. A. 2000. Enzymes: A practical introduction to structure, mechanism, and data analysis. United States: John Wiley and Sons.

Corazza, F. C., Calsavara, L. P. V., Moraes, F. F., Zanin, G. M. and Neitzel, I. 2005. Determination of inhibition in the enzymatic hydrolysis of cellobiose using hybrid neural modeling. Brazilian Journal of Chemical Engineering 22(1): 19-29.

Das, S., Bhattacharya, A., Haldar, S., Ganguly, A., Gu, S., Ting, Y. P. and Chatterjee, P. K. 2015. Optimization of enzymatic saccharification of water hyacinth biomass for bio-ethanol: Comparison between artificial neural network and response surface methodology. Sustainable Materials and Technologies 3: 17-28.

Demirhan, E., Apar, D. K. and Özbek, B. 2011. A kinetic study on sesame cake protein hydrolysis by Alcalase. Journal of Food Science 76(1): 64-67.

Dermiki, M. and FitzGerald, R. J. 2020. Physicochemical and gelling properties of whey protein hydrolysates generated at 5 and 50°C using Alcalase® and Neutrase®, effect of total solids and incubation time. International Dairy Journal 110: 104792.

Dullius, A., Fassina, P., Giroldi, M., Goettert, M. I. and Volken de Souza, C. F. 2020. A biotechnological approach for the production of branched chain amino acid containing bioactive peptides to improve human health: A review. Food Research International 131: 109002.

Gálvez, R. P., Carpio, F. J. E., Guadix, E. M. and Guadix, A. 2016. Artificial neural networks to model the production of blood protein hydrolysates for plant fertilisation. Journal of the Science of Food and Agriculture 96(1): 207-214.

Gómez Sampedro, L. J. and Zapata Montoya, J. E. 2016. Obtaining of antioxidant peptide from bovine plasma hydrolysates and effect of the degree of hydrolysis on antioxidant capacity. Revista Mexicana de Ingeniería Química 15(1): 101-109.

González-Tello, P., Camacho, F., Jurado, E., Páez, M. P. and Guadix, E. M. 1994. Enzymatic hydrolysis of whey proteins: I. Kinetic models. Biotechnology and Bioengineering 44(4): 523-528.

Haykin, S. S. 1999. Neural networks: A comprehensive foundation. United States: Prentice Hall.

Kingma, D. P. and Ba, J. L. 2015. Adam: A method for stochastic optimization. In 3rd International Conference on Learning Representations, ICLR 2015 - Conference Track Proceedings. San Diego, United States.

Marquez Moreno, M. C. and Fernandez Cuadrado, V. 1993. Enzymic hydrolysis of vegetable proteins: Mechanism and kinetics. Process Biochemistry 28(7): 481-490.

Márquez, M. C. and Vázquez, M. A. 1999. Modeling of enzymatic protein hydrolysis. Process Biochemistry 35(1-2): 111-117.

Morales-Medina, R., Pérez-Gálvez, R., Guadix, A. and Guadix, E. M. 2016. Artificial neuronal network modeling of the enzymatic hydrolysis of horse mackerel protein using protease mixtures. Biochemical Engineering Journal 105: 364-370.

Peng, Y., Rios, A., Kavuluru, R. and Lu, Z. 2018. Chemical-protein relation extraction with ensembles of SVM, CNN, and RNN models. Retrieved from website: http://arxiv.org/abs/1802.01255

Qi, W. and He, Z. 2006. Enzymatic hydrolysis of protein: Mechanism and kinetic model. Frontiers of Chemistry in China 1(3): 308-314.

Roslan, J., Yunos, K. F. M., Abdullah, N. and Kamal, S. M. M. 2014. Characterization of fish protein

hydrolysate from tilapia (*Oreochromis niloticus*) by-product. Agriculture and Agricultural Science Procedia 2: 312-319.

Samaranayaka, A. G. P. and Li-Chan, E. C. Y. 2011. Food-derived peptidic antioxidants: A review of their production, assessment, and potential applications. Journal of Functional Foods 3(4): 229-254.

Silva, F. G. D. E., Hernández-Ledesma, B., Amigo, L., Netto, F. M. and Miralles, B. 2017. Identification of peptides released from flaxseed (*Linum usitatissimum*) protein by Alcalase® hydrolysis: Antioxidant activity. LWT - Food Science and Technology 76: 140-146.

Sousa, R., Lopes, G. P., Tardioli, P. W., Giordano, R. L. C., Almeida, P. I. F. and Giordano, R. C. 2004. Kinetic model for whey protein hydrolysis by Alcalase multipoint-immobilized on agarose gel particles. Brazilian Journal of Chemical Engineering 21(2): 147-153.

Svozil, D., Kvasnička, V. and Pospíchal, J. 1997. Introduction to multi-layer feed-forward neural networks. Chemometrics and Intelligent Laboratory Systems 39(1): 43-62.

Tacias-Pascacio, V. G., Morellon-Sterling, R., Siar, E.-H., Tavano, O., Berenguer-Murcia, Á. and Fernandez-Lafuente, R. 2020. Use of Alcalase in the production of bioactive peptides: A review. International Journal of Biological Macromolecules 165: 2143-2196.

Valencia, P. L., Solis, T., Rojas, P., Ibañez, F., Astudillo-Castro, C., Pinto, M. and Almonacid, S. 2019. Proteolytic susceptibility of food by-product proteins: An evaluation by means of a quantitative index. Process Biochemistry 77: 63-69.

Valencia, P., Pinto, M. and Almonacid, S. 2014. Identification of the key mechanisms involved in the hydrolysis of fish protein by Alcalase. Process Biochemistry 49(2): 258-264.

Vasquez, P. and Zapata Montoya, J. E. 2018. Optimization of enzymatic hydrolysis of viscera proteins of rainbow trout (*Oncorhynchus mykiss*). Advance Journal of Food Science and Technology 16: 292-300.

Wu, D., Tu, M., Wang, Z., Wu, C., Yu, C., Battino, M., … and Du, M. 2020. Biological and conventional food processing modifications on food proteins: Structure, functionality, and bioactivity. Biotechnology Advances 40: 107491.